Modules of the 2024 Course



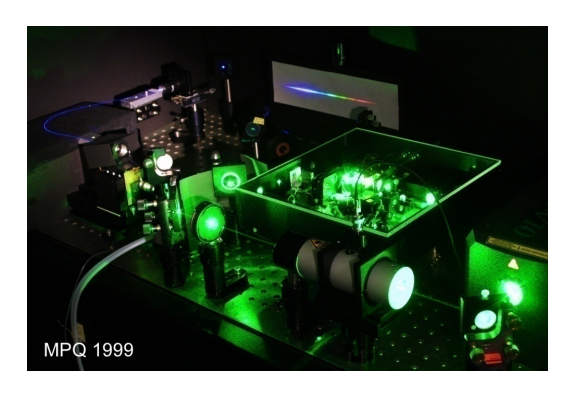
Topics covered	No	Lecture/Date
Introductory presentation; Basic of laser operation I: dispersion theory, atoms	1	11. 09. 2024
Basic of laser operation II: dispersion theory, atoms	2	18. 09. 2024
Laser systems I: 3 and 4 level lasers, gas lasers, solid state lasers, applications	3	25. 09. 2024
Laser systems II: semi-conductor lasers, external cavity lasers, applications	4	02. 10. 2024
Noise characteristics of lasers: linewidth, coherence, phase and amplitude noise, OSA (1)	5	09. 10. 2024
Noise characteristics of lasers: linewidth, coherence, phase and amplitude noise, OSA (2)	6	16. 10. 2024
Optical detection	7	30. 10. 2024
Optical fibers: light propagation in fibers, specialty fibers and dispersion (GVD)	8	06. 11. 2024
Ultrafast lasers I.: Passive mode locking and ultrafast lasers	9	13. 11. 2024
Ultrafast lasers II: mode locking, optical frequency combs / frequency metrology	10	20. 11. 2024
Ultrafast lasers III: pulse characterization, applications	11	27. 11. 2024
Nonlinear frequency conversion I: theory, frequency doubling, applications	12	04. 12. 2024
Nonlinear frequency conversion II: optical parametric amplification (OPA)	13	11. 12. 2024
Laboratory visits (lasers demo)	14	20. 12. 2024

Week 10 content



Content of Week 10

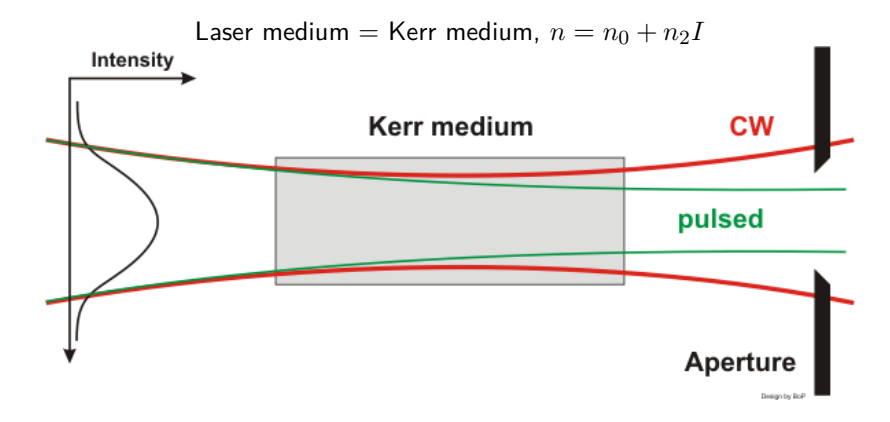
- Characterizing pulses using autocorrelation technique
- Mode locking via saturable absorbers
- Frequency Metrology
- Pulse propagation
- Dual-Comb Spectroscopy



Review: Kerr lens mode locking



Passive mode locking with Kerr lens effect



Mode locking: saturable absorber



Saturable absorber

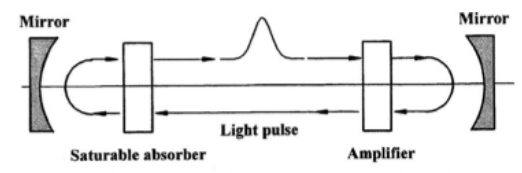
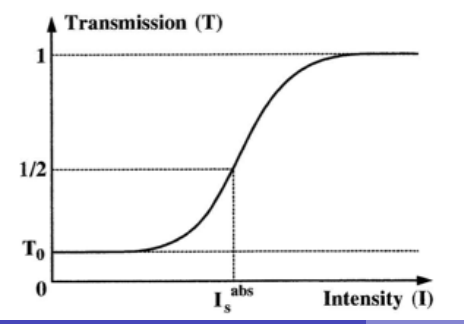
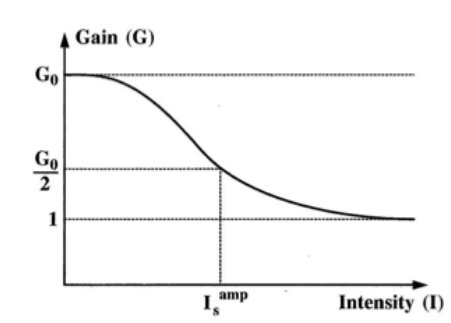


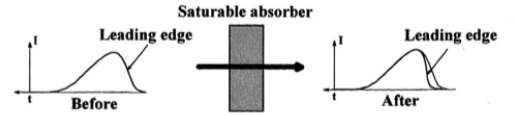
Fig. 3.12. Round-trip pulse in a laser cavity including saturable absorber and amplifying medium





Mode locking: saturable absorber





 ${\bf Fig.~3.15.}$ Illustration of pulse shape modification after crossing a saturable absorber

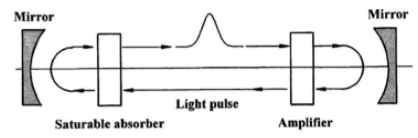


Fig. 3.12. Round-trip pulse in a laser cavity including saturable absorber and amplifying medium

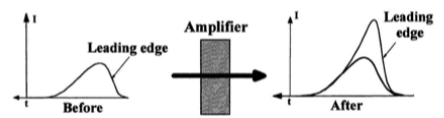
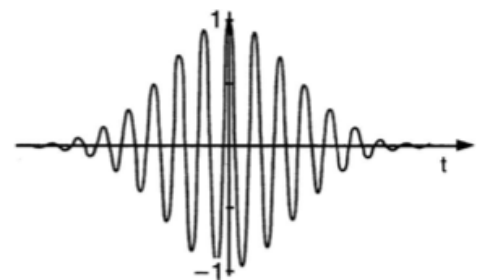


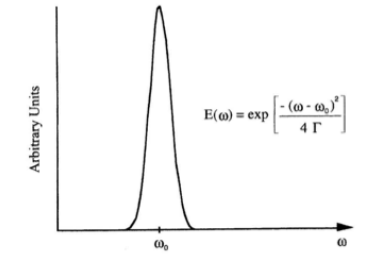
Fig. 3.16. Illustration of pulse shape modification after crossing an amplifying medium

One Gaussian Pulse





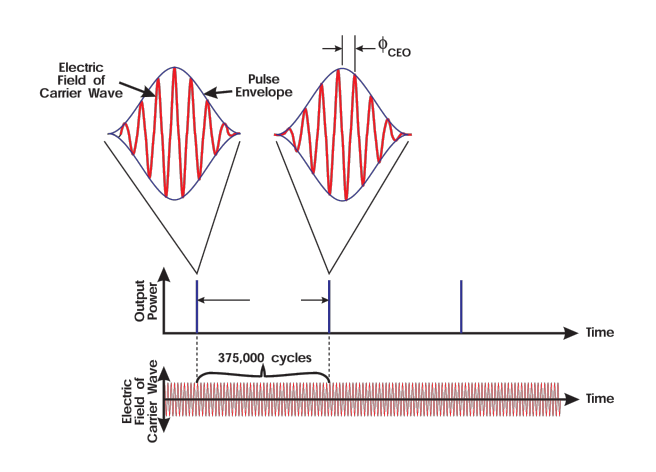
$$E_P(t) = E_0 e^{-\Gamma t^2 + i\omega_0 t}$$



$$\tilde{E}_p(\omega) = E_0 \sqrt{\frac{\pi}{\Gamma}} \exp\left(\frac{-(\omega - \omega_0)^2}{4\Gamma}\right)$$

Gaussian Pulse Train with Phase 'Slip'





Per-pulse change of phase:

$$\begin{split} \Delta \phi &= \beta_0 L - \omega_0 T_{\text{rep}} \\ &= \beta_0 L - \frac{\omega_0 L}{v_g} \\ &= \omega_0 L \left(\frac{\beta_0}{\omega_0} - \frac{1}{v_g} \right) \\ &= \frac{\omega_0 L}{c} \left(n_0 - n_g \right) \end{split}$$

The group-index

$$n_g = n_0 + \omega_0 \frac{dn}{d\omega} \bigg|_{\omega_0}$$

Phase change per time: the carrier-envelope offset frequency

$$\omega_{\rm CO} = \frac{\Delta \phi}{T_{\rm rep}}$$

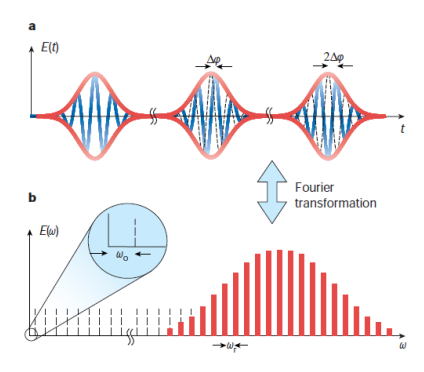
Carrier Envelope Frequency



$$E_T(t) = \sum_{m=0}^{N-1} E_P(t - mT_{\text{rep}}) e^{-i\omega_{\text{CO}}t}, \quad \omega_{\text{CO}} = \frac{\Delta\phi}{T_{\text{rep}}}$$

$$\tilde{E}_T(\omega) = \text{FT}\left[E_T(t)\right] = \sum_{m=0}^{N-1} \int_{-\infty}^{\infty} E_P(t - mT_{\text{rep}}) e^{-i\omega_{\text{CO}}t} e^{-i\omega t} dt$$

Translation property: unreadable (duality)



$$\begin{split} I_T(\omega) &= I_P \left(\omega + \omega_{\text{CO}} \right) \frac{1 - \cos \left(2N\pi \left(\omega + \omega_{\text{CO}} \right) / \omega_{\text{rep}} \right)}{1 - \cos \left(2\pi \left(\omega + \omega_{\text{CO}} \right) / \omega_{\text{rep}} \right)} \\ &= \tilde{E}_P \left(\omega + \omega_{\text{CO}} \right) \frac{1 - e^{-iNT_{\text{rep}} \left(\omega + \omega_{\text{CO}} \right)}}{1 - e^{-iT_{\text{rep}} \left(\omega + \omega_{\text{CO}} \right)}} \end{split}$$

$$\omega_{
m rep} = rac{2\pi}{T_{
m rep}}$$

$$I_T(\omega) = I_P\left(\omega + \omega_{\mathrm{CO}}\right) rac{1 - \cos\left(2N\pi\left(\omega + \omega_{\mathrm{CO}}\right)/\omega_{\mathrm{rep}}\right)}{1 - \cos\left(2\pi\left(\omega + \omega_{\mathrm{CO}}\right)/\omega_{\mathrm{rep}}\right)}$$

$$\lim_{N\to\infty} I_T(\omega) = I_P(\omega + \omega_{\text{CO}}) \sum_{m=-\infty}^{\infty} \delta\left(\omega + \omega_{\text{CO}} - m\omega_{\text{rep}}\right)$$

A frequency comb with offset $\omega_{\rm CO}$

Reverse Quick Method



Starting from offset frequency comb:

$$\tilde{E}_T(\omega) = \tilde{E}_P(\omega) \sum_{m=-\infty}^{\infty} \delta(\omega + \omega_{\text{CO}} - m\omega_{\text{rep}})$$

FT of multiplication = convolution of FT:

$$E_T(t) = \mathrm{FT}\left[\tilde{E}_P(\omega)\right] \# \mathrm{FT}\left[\sum_{m=-\infty}^{\infty} \delta\left(\omega + \omega_{\mathrm{CO}} - m\omega_{\mathrm{rep}}\right)\right]$$

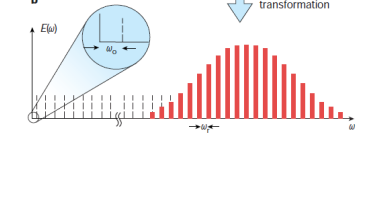
FT of Dirac Comb = Dirac Comb:

$$= E_P(t) \# \left[\sum_{m=-\infty}^{\infty} \delta \left(t - m T_{\text{rep}} \right) e^{-i\omega_{CO} t} \right]$$

Convolution with Dirac Comb = "Replicating Property"

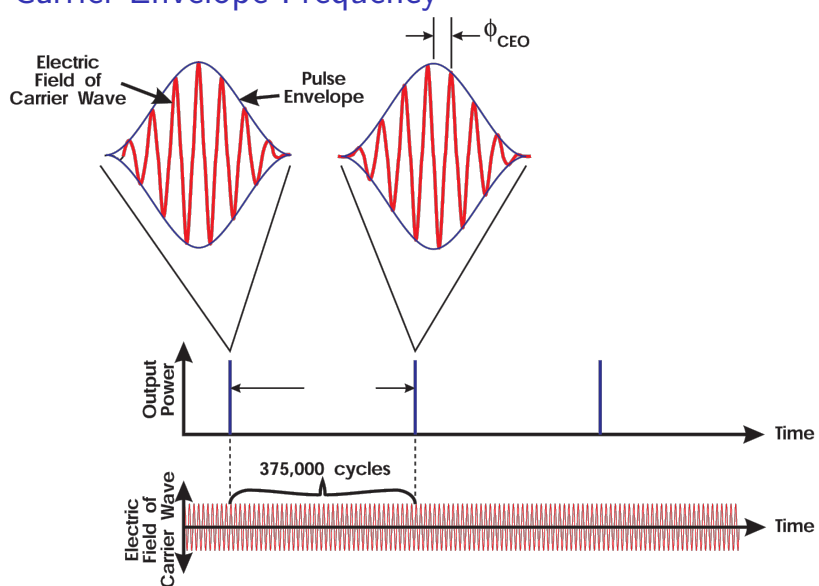
$$= \sum_{m=-\infty}^{\infty} E_P (t - mT_{\text{rep}}) e^{-im\Delta\phi}$$

Back to our original pulse-train



Carrier Envelope Frequency



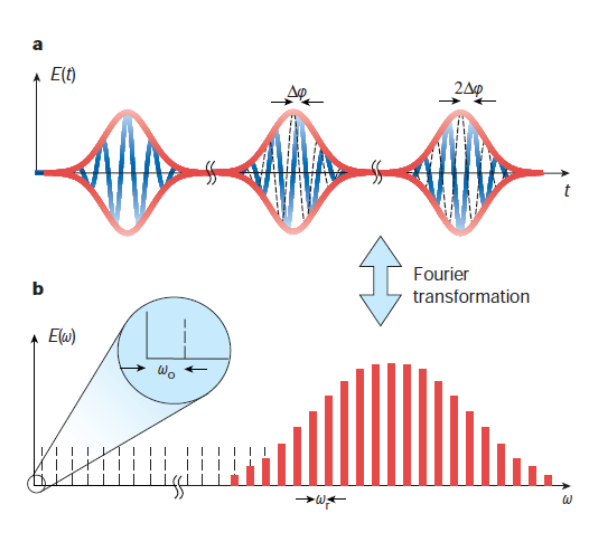


$$u_{\text{CEO}} = \frac{d\Phi}{dt} = \frac{\Delta\Phi}{2\pi T}$$

$$\nu_m = m f_{\rm rep} + \nu_{\rm CEO}$$

Carrier Envelope Frequency



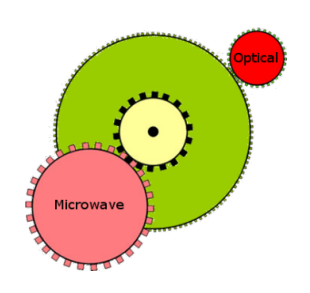


Applications of ultra-short pulses: Optical Clocks



Optical atomic clocks (NIST, Boulder, Colorado)

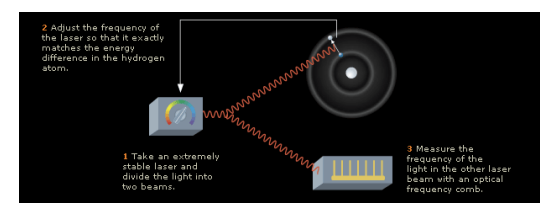








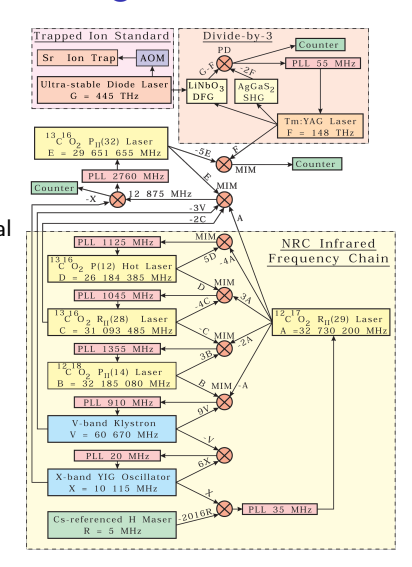




Counting the cycles of light



Figure 3: The NRC classical chain for measuring the optical transition at 445 THz in a single trapped strontium ion.



VOLUME 76, NUMBER 1 PHYSICAL REVIEW LETTERS 1 JANUARY 1996

First Phase-Coherent Frequency Measurement of Visible Radiation

H. Schnatz, B. Lipphardt, J. Helmcke, F. Riehle, and G. Zinner

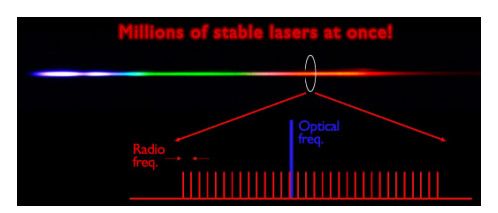
Physikatisch-Technische Bundesonnatt (PTB), D-38116 Braunschweig, Germany

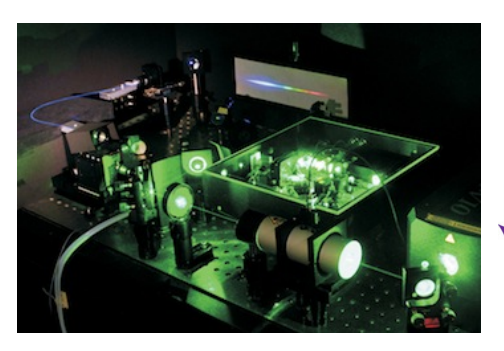
(Received 10 August 1995)

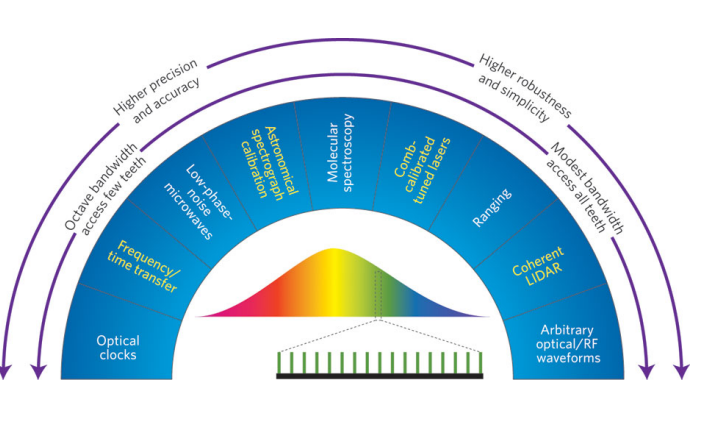


Applications of frequency combs



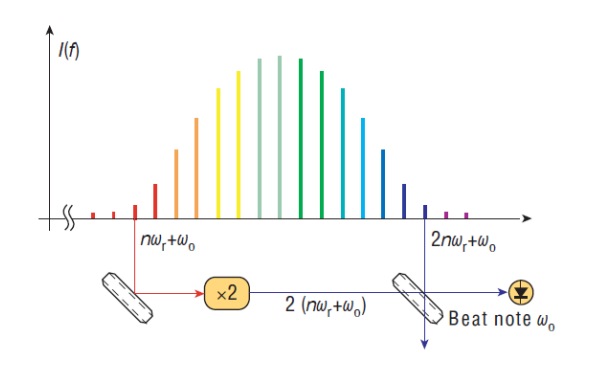






Measuring the carrier envelope frequency



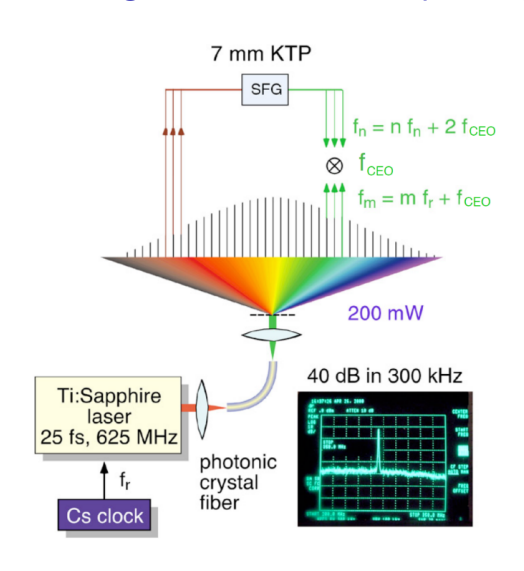


$$f_n = nf_{\text{rep}} + f_0$$

$$2f_n - f_{2n} = 2(nf_{rep} + f_0) - (2nf_{rep} + f_0) = f_0$$

Measuring the carrier envelope frequency







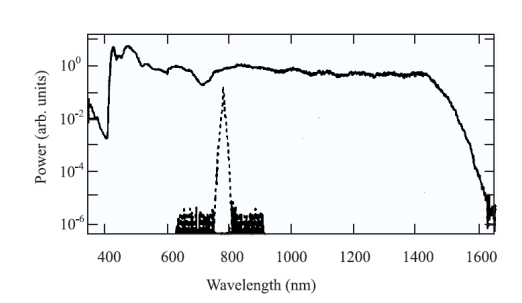


"Rainbow Fiber"

"Photonic Crystal Fiber"

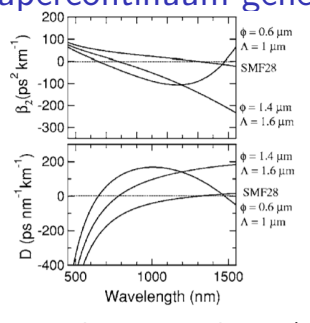
(Lucent Technologies, 1999)

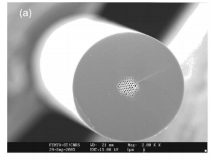
J.C. Knight, W.J. Wadsworth, P. St. Russel University of Bath, UK



Supercontinuum generation







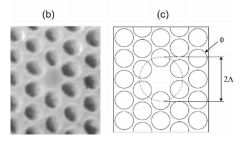


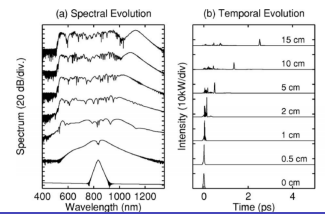
FIG. 2. Calculated GVD parameter β_2 (top) and D (bottom) for PCFs with parameters as shown: $\Lambda=1~\mu m,~\phi=0.6~\mu m;$ $\Lambda=1.6~\mu m,~\phi=1.4~\mu m$ [that used by Ranka et al. (2000a)]; and standard Corning SMF28 single-mode fiber.

REVIEWS OF MODERN PHYSICS, VOLUME 78, OCTORER_DECEMBER 2006

Supercontinuum generation in photonic crystal fiber

Super-continuum generation can be modeled via a generalized Nonlinear Schrödinger equation.

$$\frac{dA}{dz} + \frac{\alpha}{2}A - \sum_{k \geq 2} \frac{i^{k+1}}{k!} \beta_k \frac{\partial^k A}{\partial T^k} = i\gamma \left(1 + i\tau \frac{\partial}{\partial T}\right) \cdot \left(A(z,T) \int_{-\infty}^{\infty} R\left(T'\right) \left|A\left(z,T - T'\right)\right|^2 dT' + i\Gamma_R(z,T)\right)$$

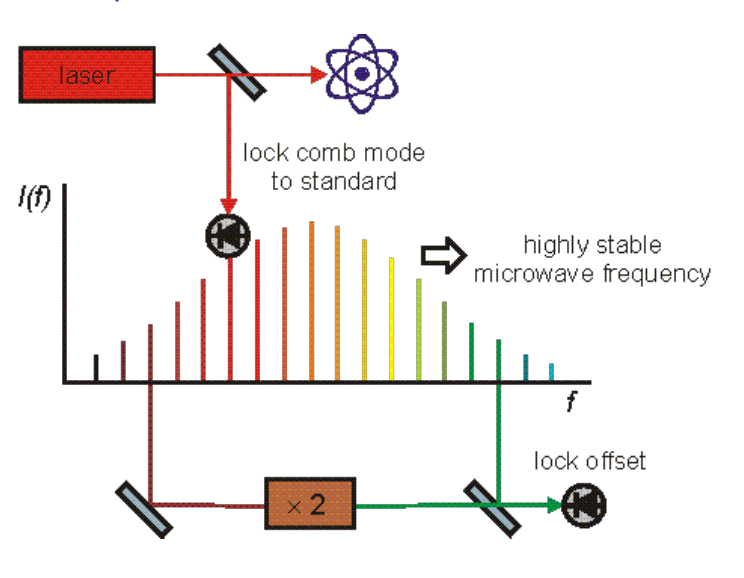






Principle of an atomic clock





Optical atomic clock: state of the art



An Optical Clock Based on a Single Trapped ¹⁹⁹Hg⁺ Ion

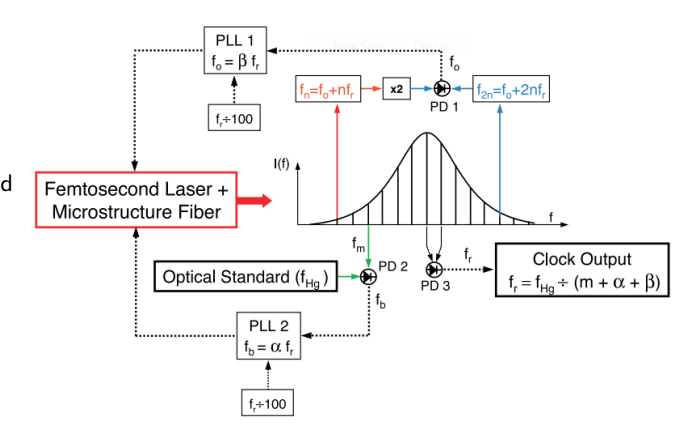
S. A. Diddams, 1* Th. Udem, 1† J. C. Bergquist, 1 E. A. Curtis, 1.2
R. E. Drullinger, 1 L. Hollberg, 1 W. M. Itano, 1 W. D. Lee, 1
C. W. Oates, 1 K. R. Vogel, 1 D. J. Wineland 1



A clockwork based on a mode-locked femtosecond laser provides output pulses at a 1-gigahertz rate that are phase-coherently locked to the optical frequency. By comparison to a laser-cooled calcium optical standard, an upper limit for the fractional frequency instability of $7 \cdot 10^{-15}$ is measured in 1 second of averaging — a value substantially better than that of the world's best microwave atomic clocks

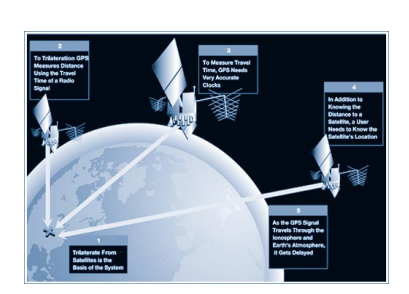
Fractional frequency instability:

$$\sigma_y(\tau) \approx \left\langle \frac{\Delta \nu_{\rm rms}}{\nu_0} \right\rangle_{\tau}$$



Atomic clocks





1999 – NIST-F1 begins operation with an uncertainty of $1.7 \cdot 10^{-15}$, or accuracy to about one second in 20 million years, making it one of the most accurate clocks ever made (a distinction shared with similar standards in France and Germany).





Three spheres are necessary to find position in two dimensions, four are needed in three dimensions.

Best clocks to date



Optical Clocks and Relativity

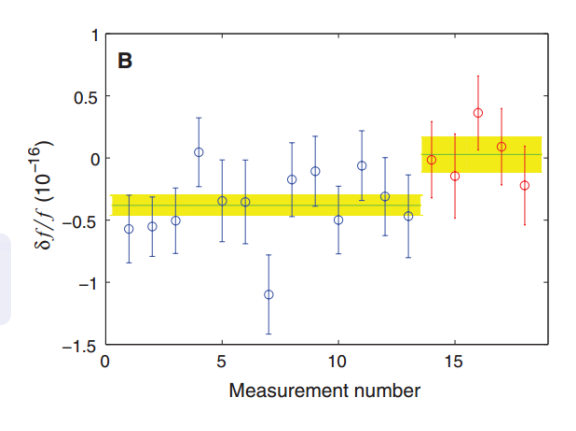
C. W. Chou.* D. B. Hume, T. Rosenband, D. 1. Wineland

Observers in relative motion or at different gravitational potentials measure disparate clock rates. These predictions of relativity have previously been observed with atomic clocks at high velocities and with large changes in elevation. We observed time dilation from relative speeds of less than 10 meters per second by comparing two optical atomic clocks connected by a 75-meter length of optical fiber. We can now also detect time dilation due to a change in height near Earth's surface of less than 1 meter. This technique may be extended to the field of geodesy, with applications in geophysics and hydrology as well as in space-based tests of fundamental physics.



$$\sigma_y(au) pprox \left\langle \frac{\Delta v_{
m rms}}{v_0} \right\rangle_{ au}$$

Gravitational time dilation at the scale of daily life. (A) As one of the clocks is raised, its rate increases when compared to the clock rate at deeper gravitational potential



Autocorrelation techniques



How can a fast temporal profile of a few fs be measured?

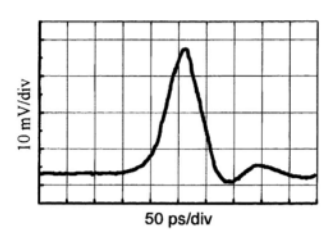
Direct electronic means are too slow

1

All optical means

Table 7.2. Examples of data from photodiodes (Antel)

Model (Si PIN)	Rise time [ps]		-3dB Bandwith [GHz]	Responsivity [V/W]	Responsivity (in terms of density) [V/(W/mm ²)]
AR-S1	< 100	< 180	> 3.5	16	4
AR-S2	< 35	< 65	> 10	5	0.018
AR-S3	< 25	< 45	> 14	3.75	0.014



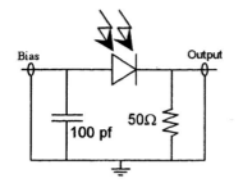


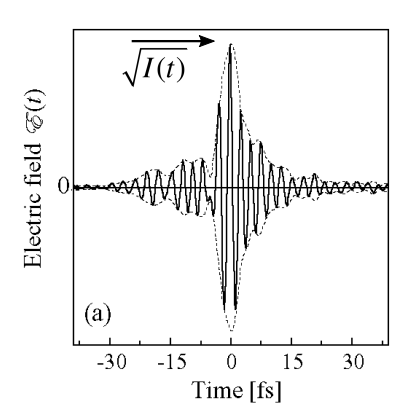
Fig. 7.3. Typical electrical signal given by a photodiode (Antel AR-S2) in response to a femtosecond laser pulse, and the corresponding electric circuit

Pulse characterization



Neglecting the spatial dependence for now, the pulse electric field is given by:

$$E(t) = \operatorname{Re} \left\{ \sqrt{I(t)} \underbrace{\exp}_{\text{Intensity}} \left\{ i \left[\underbrace{\omega_0}_{\text{0}} t - \underbrace{\phi(t)}_{\text{Phase}} \right] \right\} \right\}$$



Chirped pulses



$$E_y = \operatorname{Re}\left(E_0 e^{\left(-\Gamma t^2 + i\omega_0 t\right)}\right)$$



$$E_y = \operatorname{Re}\left(E_0 e^{\left[-\Gamma t^2 + i\left(\omega_0 t - at^2\right)\right]}\right)$$



Instantaneous frequency:

Instantaneous frequency:

The pulse is said to be "chirped"

Pulse propagation through media



$$E_{0}(\omega) = e^{\frac{-(\omega - \omega_{0})^{2}}{4\Gamma}} \quad E(\omega, x) = E_{0}(\omega)e^{\pm ik(\omega)x}, \quad k(\omega) = \frac{n\omega}{c}$$

$$k(\omega) = k(\omega_{0}) + k'(\omega - \omega_{0}) + \frac{1}{2}k''(\omega - \omega_{0})^{2} + \dots$$

$$E(\omega, x) = \exp\left[-ik(\omega_{0})x - ikx(\omega - \omega_{0}) - \left(\frac{1}{4\Gamma} + \frac{i}{2}k''\right)(\omega - \omega_{0})^{2}\right]$$

$$\varepsilon(t, x) = -\frac{1}{\pi^{2}} \int_{-\infty}^{+\infty} E(\omega, x)e^{i\omega t}d\omega$$

$$\varepsilon(t, x) = \sqrt{\frac{\Gamma(x)}{\pi}} \exp\left[i\omega_{0}\left(t - \frac{x}{\nu_{\phi}(\omega_{0})}\right)\right] \times \exp\left[-\Gamma(x)\left(t - \frac{x}{\nu_{g}(\omega_{0})}\right)^{2}\right]$$

Pulse propagation through media



$$\omega_{\phi}(\omega_{0}) = \left(\frac{\omega}{k}\right)_{\omega_{0}}$$

$$v_{g}(\omega_{0}) = \left(\frac{d\omega}{dk}\right)_{\omega_{0}}$$

$$v_{g} < v_{\phi}$$

$$\nu_{\phi}(\omega_{0}) = \left(\frac{\omega}{k}\right)_{\omega_{0}}, \quad \nu_{g}(\omega_{0}) = \left(\frac{d\omega}{dk}\right)_{\omega_{0}}, \quad \frac{1}{\Gamma(x)} = \frac{1}{\Gamma} + 2ik''x$$

$$\nu_{\phi} = \frac{c}{n(\omega)}$$

$$\nu_g = \frac{d\omega}{dk} = \frac{1}{dk/d\omega},$$

$$\frac{dk}{d\omega} = \frac{1}{c} \left(n(\omega) + \omega \frac{dn(\omega)}{d\omega} \right)$$

$$u_g \approx \nu_\phi \left(1 - \frac{\omega}{n(\omega)} \frac{dn(\omega)}{d\omega} \right)$$

Group and phase velocity



Slowing of light pulses

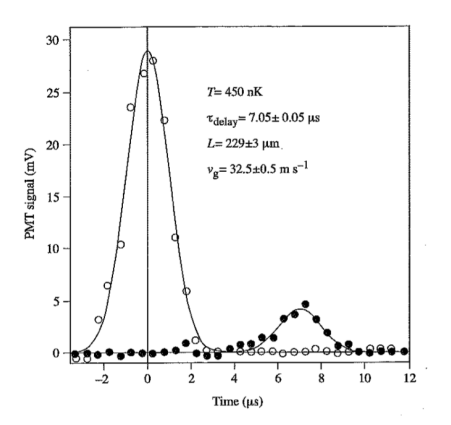
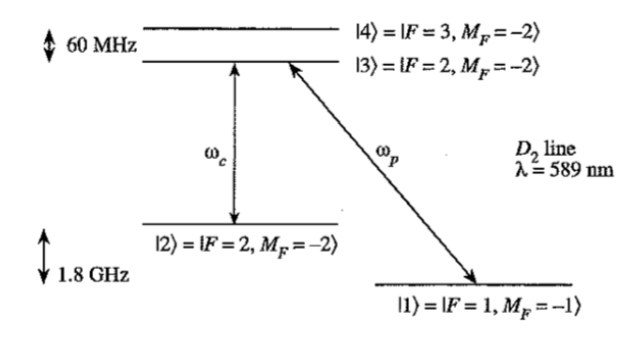


Figure 5.6. Experimental data of Hau *et al* showing the input pulse (open circles) and the pulse transmitted by an ultracold gas of length $229 \pm 3 \mu m$ (filled circles). The transmitted pulse delay of $7.05 \pm 0.05 \mu s$ corresponds to a group velocity of $32.5 \pm 0.5 m s^{-1}$. From 1791, with permission.



Group and phase velocity



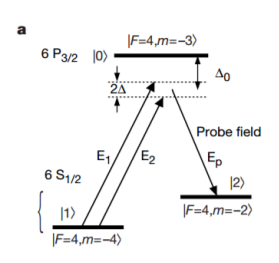
Superluminal group velocity

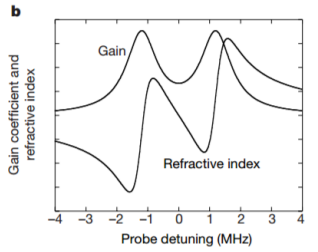
Gain-assisted superluminal light propagation

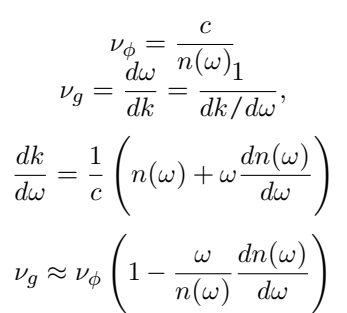
L. J. Wang, A. Kuzmich & A. Dogariu

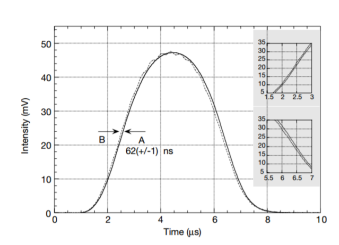
NEC Research Institute, 4 Independence Way, Princeton, New Jersey 08540, USA

Einstein's theory of special relativity and the principle of causality1-4 imply that the speed of any moving object cannot exceed that of light in a vacuum (c). Nevertheless, there exist various proposals⁵⁻¹⁸ for observing faster-than-c propagation of light pulses, using anomalous dispersion near an absorption line^{4,6-8}, nonlinear⁹ and linear gain lines¹⁰⁻¹⁸, or tunnelling barriers¹⁹. However, in all previous experimental demonstrations, the light pulses experienced either very large absorption⁷ or severe reshaping 9,19, resulting in controversies over the interpretation. Here we use gain-assisted linear anomalous dispersion to demonstrate superluminal light propagation in atomic caesium gas. The group velocity of a laser pulse in this region exceeds c and can even become negative 16,17, while the shape of the pulse is preserved. We measure a group-velocity index of $n_{\rm e}=-310(\pm 5)$; in practice, this means that a light pulse propagating through the atomic vapour cell appears at the exit side so much earlier than if it had propagated the same distance in a vacuum that the peak of the pulse appears to leave the cell before entering it. The observed superluminal light pulse propagation is not at odds with causality. being a direct consequence of classical interference between its different frequency components in an anomalous dispersion region.









Energy propagation velocity



Energy propagation velocity

$$|S_{\omega}| = \frac{n}{2\mu c} |E_{\omega}|^2 = \nu_g u_{\omega}$$
$$v_E \equiv |S_{\omega}| / u_{\omega}$$

Electron oscillator model:

$$\begin{split} m\left(\ddot{r}+\Gamma\dot{r}+\omega_0^2r\right) &= eE\\ \nu_E &= \frac{c}{n_R+2\omega n_I/\Gamma} = \frac{\nu_p}{1+2\omega n_I/n_R\Gamma} \end{split}$$

Lossless limit:

$$\nu_E = c \left[n_R + \frac{\omega^2 \omega_p^2 / n_R}{\left(\omega_0^2 - \omega^2\right)^2} \right]^{-1} = \frac{c}{n_R + \omega \cdot dn_R / d\omega} = v_g$$



The speed of information in a 'fast-light' optical medium

Michael D. Stenner¹, Daniel J. Gauthier¹ & Mark A. Neifeld

¹Duke University, Department of Physics, and The Fitzpatrick Center for Photonics and Communication Systems, Durham, North Carolina 27708, US ²Department of Electrical and Computer Engineering, The Optical Sciences

One consequence of the special theory of relativity is that no signal can cause an effect outside the source light cone, the space time surface on which light rays emanate from the source' Violation of this principle of relativistic causality leads to paradoxes, such as that of an effect preceding its cause'. Recent experiments on optical pulse propagation in so-called 'fastlight' media achieb are characterized by a serve group velocity r, exceeding the vacuum speed of light c or taking on negative values!—have led to renessed debate about the definition of the information velocity v_i . One view is that $v_i \equiv v_{\sigma}$ (ref. 4), which would violate causality, while another is that v, = c in all situations', which would preserve causality. Here we find that the time to detect information propagating through a fast-light medium is slightly longer than the time required to detect the same information travelling through a vacuum, even though r, in the medium vastly exceeds c. Our observations are therefore consistent with relativistic causality and help to resolve the controversies surrounding superluminal pulse propagation.

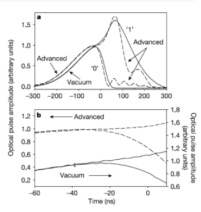


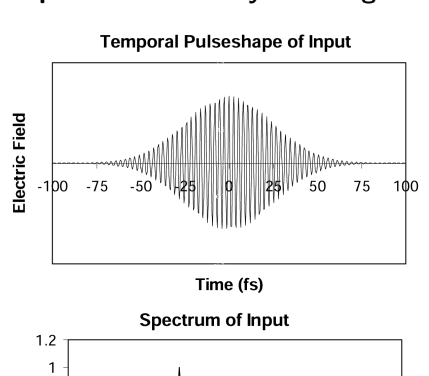
Figure 2 incommittry interaction exceeded optical pales intrough is saidly involved.

A ill amounting 1 and 1 figure, the last effective data which led and vices and led the facility for solid. The figure is the saidly read to the facility of the saidly read to the facility of the figure is the saidly read of a similar and the color. If the saidly file and pales is depressed and the first backers of an interaction of the saidly read of the saidly

Autocorrelation techniques



Example of pulse distortion by traveling through glass



Spectrum of Input

1.2

1.2

0.8

0.6

0.4

0.2

400

600

800

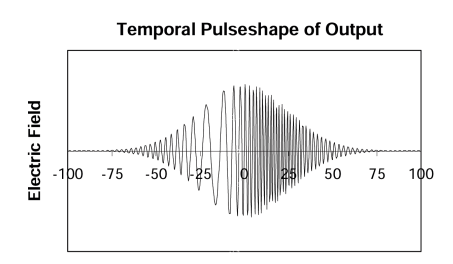
1000

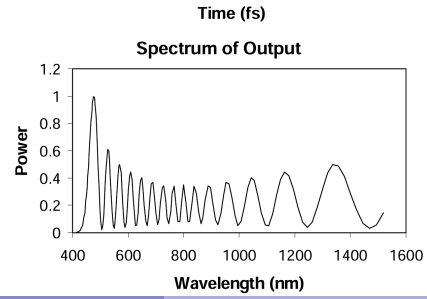
1200

1400

1600

Wavelength (nm)



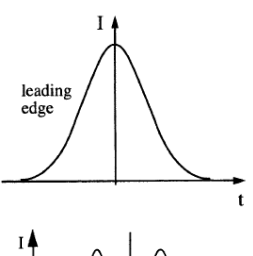


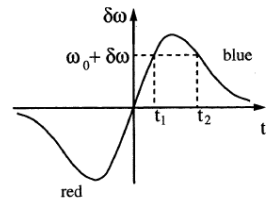
Autocorrelation techniques



What can give rise to chirped pulses?

$$\delta\omega(t) = \omega(t) - \omega_0 = -\frac{\omega_0 n_2}{2c} x \frac{\partial I(t)}{\partial t}$$





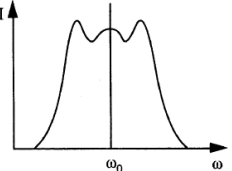


Fig. 2.19. Frequency spectrum of an originally Gaussian pulse which has suffered an induced phase shift equal to 2π

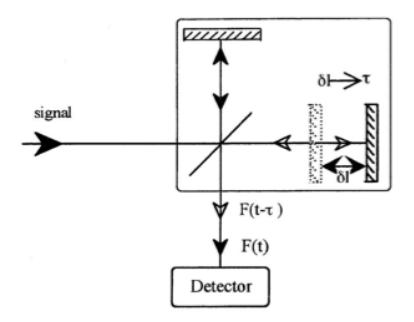
Autocorrelation



All optical Pulse characterization techniques are based on time to space transformations. 1 ps \leftrightarrow 300 μ m in air

7.4.2 & 7.5 (Ruliere, "femtosecond laser pulses") How to measure characteristics of laser pulses

$$I_1(\tau) = \int_{-\infty}^{+\infty} |E(t) + E(t - \tau)|^2 dt$$
$$I_1(\tau) \propto 2 \int I(t) dt + 2G(\tau)$$



Second order autocorrelation

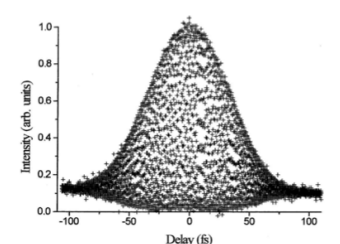


$$I_2(\tau) = \int_{-\infty}^{+\infty} \left| \left\{ E(t)e^{i[\omega t + \Phi(t)]} + E(t - \tau)e^{i[\omega(t - \tau) + \Phi(t - \tau)]} \right\}^2 \right|^2 dt$$

$$I_{2}(\tau) = \int_{-\infty}^{+\infty} |2E^{4} + 4E^{2}(t)E^{2}(t - \tau)$$

$$+ 4E(t)E(t - \tau) \left[E^{2}(t) + E^{2}(t - \tau) \right] \cos[\omega \tau + \Phi(t) - \Phi(t - \tau)]$$

$$+ 2E^{2}(t)E^{2}(t - \tau) \cos[2(\omega \tau + \Phi(t) - \Phi(t - \tau))] |dt$$



$$I_2(\tau = 0) = 2^4 \int E^4(t)dt$$
$$I_2(\tau \to \infty) = 2 \int E^4(t)dt$$

Second order autocorrelation



Fringes are spatially averaged (same effect as fast sweep)

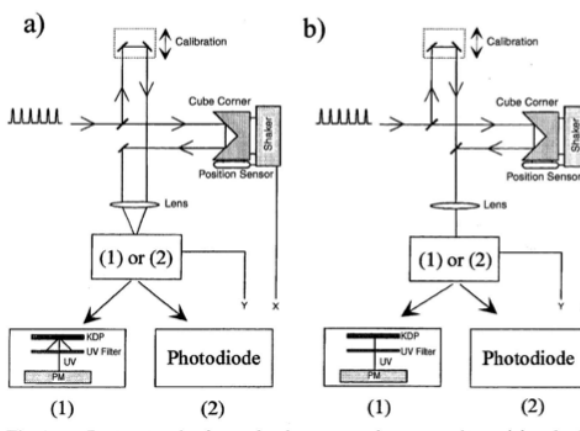
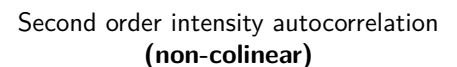
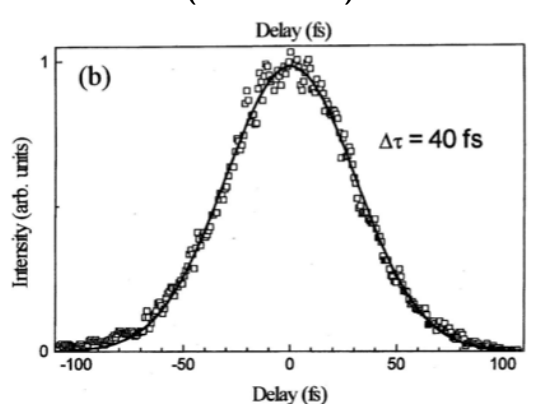


Fig. 7.13. Basic principle of second-order autocorrelator: noncolinear (a) and colinear (b) arrangements

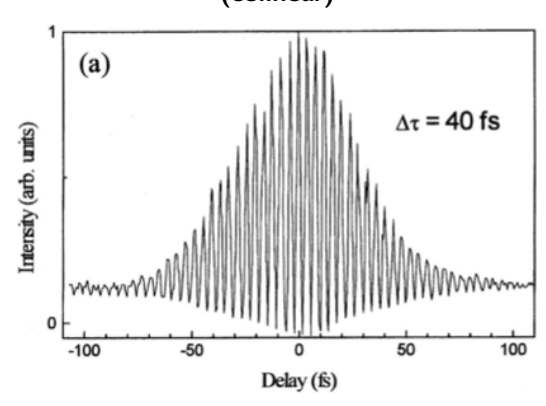
Second order autocorrelation





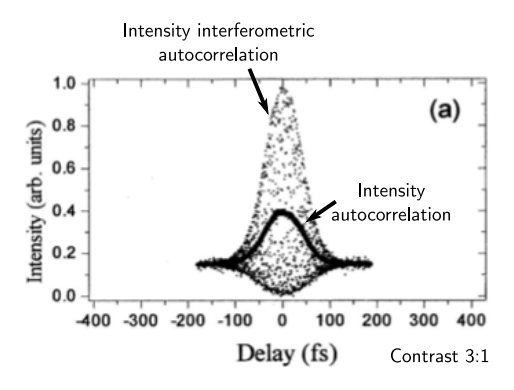


Second order interferometric autocorrelation (colinear)



Interferometric vs. Intensity 2nd Order Autocorr.

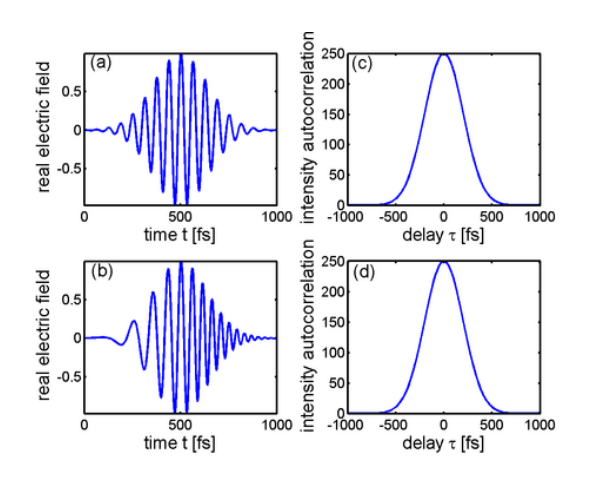




$$I_2(\tau) = \int_{-\infty}^{+\infty} \left| \left\{ E(t)e^{i[\omega t + \Phi(t)]} + E(t - \tau)e^{i[\omega(t - \tau) + \Phi(t - \tau)]} \right\}^2 \right|^2 dt$$
$$G_2(\tau) = \frac{\int_{-\infty}^{+\infty} I(t)I(t - \tau)dt}{\int_{-\infty}^{+\infty} I^2(t)dt}$$

Second-order Autocorrelation

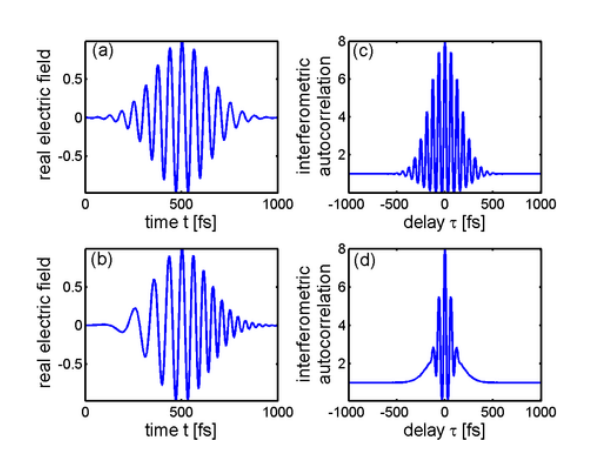




Two ultrashort pulses (a) and (b) with their respective intensity autocorrelation (c) and (d). Because the intensity autocorrelation ignores the temporal phase of pulse (b) that is due to the instantaneous frequency sweep (chirp), both pulses yield the same intensity autocorrelation. The zero in this figure has been shifted to omit this background.

Second-order Autocorrelation





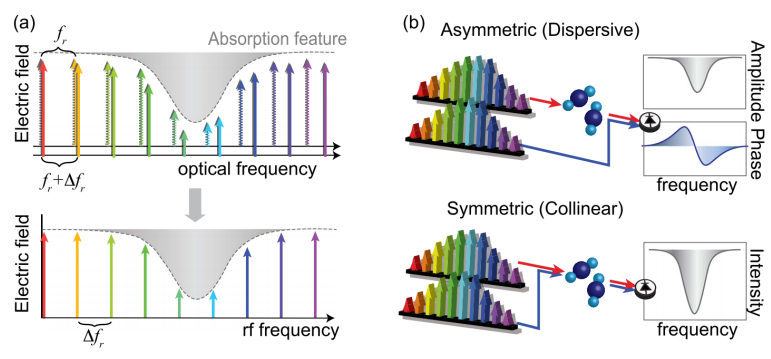
Two ultrashort pulses (a) and (b) with their respective interferometric 2nd order autocorrelation (c) and (d). Because of the phase present in pulse (b) due to an instantaneous frequency sweep (chirp), the fringes of the autocorrelation trace (d) wash out in the wings. Note the ratio 8:1 (peak to the wings), characteristic of interferometric autocorrelation traces.

Dual-Comb Spectroscopy (DCS)



Can we apply frequency comb for spectroscopy measurements?

Comb light could be coupled into conventional spectrometers. However, since the comb tooth spacing is finer than the resolution of nearly all spectrometers. Its associated frequency resolution and accuracy are lost! \rightarrow Let's apply Dual-Comb and transfer signal to RF domain!



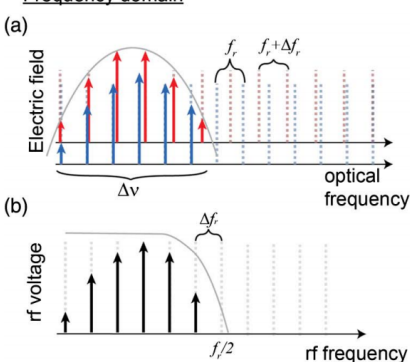
Dual-comb spectroscopy

IAN CODDINGTON, 1,* NATHAN NEWBURY, 1,2 AND WILLIAM SWANN 1

Dual-Comb Spectroscopy (DCS)

EPFL

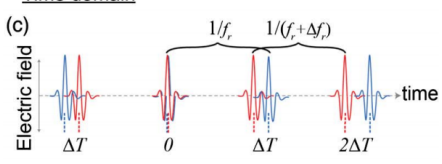
Frequency domain

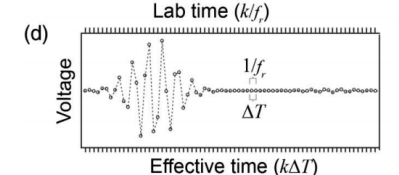


$$m = f_r / \Delta f_r$$

$$\Delta \nu \le m f_r / 2 = f_r^2 / (2\Delta f_r)$$

Time domain





$$\Delta T = \frac{\Delta f_r}{f_r \left(f_r + \Delta f_r \right)} \approx \frac{1}{m f_r}$$

The minimum time to resolve the RF comb teeth, and therefore acquire a single spectrum, is simply $\frac{1}{\Lambda f_a}$.

Dual-Comb Spectroscopy (DCS)



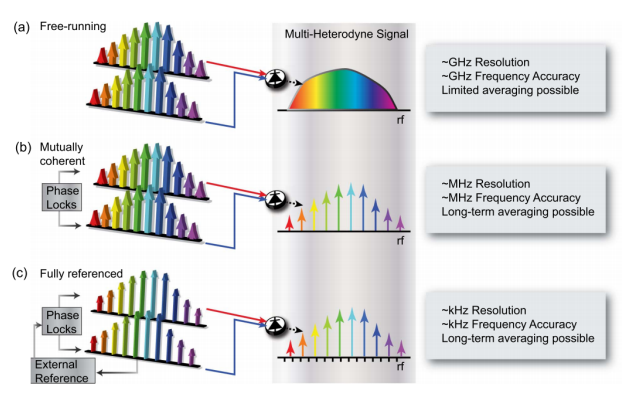
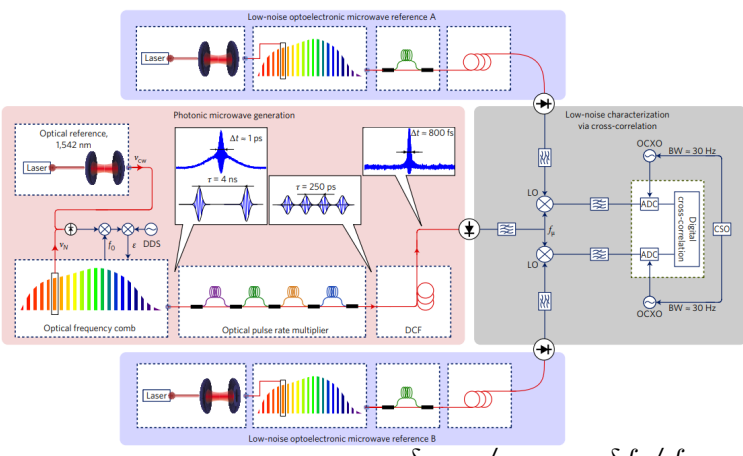


Fig. 4. Three different categories of DCS demonstrations. (a) Free-running combs can yield dual-comb spectra, but with low resolution, low frequency accuracy, and low SNR, since only limited signal averaging is possible; (b) mutually coherent combs can yield comb-tooth-resolved spectra that can be averaged for high SNR; and (c) fully referenced combs yield spectra with simultaneous high resolution, absolute frequency accuracy, and high SNR. Text boxes indicate some general rules of thumb for frequency combs based on mode-locked lasers.

Optical to microwave frequency division





 $\delta \nu_{\rm CW} / \nu_{\rm CW} = \delta f_{\rm r} / f_{\rm r} = \delta f_{\mu} / f_{\mu}$

Figure 1 | Experimental set-up for low-noise microwave generation and characterization. The left part of the set-up is used to generate a record low-noise 12 GHz microwave signal from an ultrastable optical reference at 1.542 nm via optical division. The right part is used to characterize the microwave-signal phase noise using a heterodyne digital cross-correlation method. The auxiliary optoelectronic microwave references A and 8 are also obtained by low-noise optical division of the light from two additional distinct ultrastable laser references at 1.542 nm using two separate optical frequency combs. ADC, analog-to-digital converter; CSO, cryogenic sapphire oscillator; CFC, dispersion compensation fifter DDS, direct digital synthesizer, Octow-controlled crystal oscillator.

Fiber laser mode locking



All polarization-maintaining fiber laser architecture for robust femtosecond pulse generation

